PHILOSOPHICAL TRANSACTIONS OF THE ROYAL SOCIETY B BIOLOGICAL SCIENCES

Properties of fast endocytosis at hippocampal synapses

Ege T. Kavalali, Jürgen Klingauf and Richard W. Tsien

Phil. Trans. R. Soc. Lond. B 1999 **354**, 337-346
doi: 10.1098/rstb.1999.0385

THE ROYAL SOCIETY

Properties of fast endocytosis at hippocampal synapses

Ege T. Kavalali†, Jürgen Klingauf† and Richard W. Tsien*

Department of Molecular and Cellular Physiology, Stanford Medical Center, Stanford, CA 94305, USA

Regulation of synaptic transmission is a widespread means for dynamic alterations in nervous system function. In several cases, this regulation targets vesicular recycling in presynaptic terminals and may result in substantial changes in efficiency of synaptic transmission. Traditionally, experimental accessibility of the synaptic vesicle cycle in central neuronal synapses has been largely limited to the exocytotic side, which can be monitored with electrophysiological responses to neurotransmitter release. Recently, physiological measurements on the endocytotic portion of the cycle have been made possible by the introduction of styryl dyes such as FM1-43 as fluorescent markers for recycling synaptic vesicles. Here we demonstrate the existence of fast endocytosis in hippocampal nerve terminals and derive its kinetics from fluorescence measurements using dyes with varying rates of membrane departitioning. The rapid mode of vesicular retrieval was greatly speeded by exposure to staurosporine or elevated extracellular calcium. The effective time-constant for retrieval can be <2 seconds under appropriate conditions. Thus, hippocampal synapses capitalize on efficient mechanisms for endocytosis and their vesicular retrieval is subject to modulatory control.

Keywords: endocytosis; synapse; hippocampus; fluorescence imaging; FM1-43

1. INTRODUCTION

Various modes of vesicle recycling must be considered at central nervous system (CNS) synapses, based on work in other systems (see Henkel & Almers 1996, for review). In the classical endocytotic pathway (figure 1), vesicles collapse completely into the surface membrane, internalize slowly (>20 s), then recycle through the endosome (Heuser & Reese 1973; Miller & Heuser 1984; Koenig & Ikeda 1996). Vesicles may also reform directly by uncoating of clathrin-coated vesicles without equilibration with endosomes (Takei *et al*. 1996). In a more rapid endocytotic pathway, generally known as 'kiss and run' (Ceccarelli *et al*. 1973; Ceccarelli & Hurlbut 1980; Fesce *et al*. 1994), vesicles are rapidly retrieved after short-lived fusion pore openings (Ceccarelli & Hurlbut 1980; Fesce *et al*. 1994; Henkel & Betz 1995; Koenig & Ikeda 1996; Murthy & Stevens 1998). In the 'kiss and run' pathway, synaptic vesicles would retain their complex molecular composition and therefore be swiftly handled throughout the cycle during wide range of stimuli. Thus, this mechanism provides an attractive alternative to more classical vesicle recycling schemes.

The kinetics and mechanisms of vesicular endocytosis and repriming are of particular interest at synapses between central neurons (Betz *et al*. 1996; Ryan *et al*. 1996; Cremona & De Camilli 1997). Because these presynaptic terminals contain no more than a few hundred vesicles (Harris & Sultan 1995; Schikorski & Stevens 1997), they must recycle them soon after they undergo exocytosis in order to preserve synaptic transmission and presynaptic morphology during repetitive firing (Betz *et al*. 1996; Ryan *et al*. 1996). Vesicles in hippocampal nerve terminals can become available to release their contents within *ca*. 40 s after a prior round of exocytosis (Ryan *et al*. 1993, 1996; Liu & Tsien 1995; Lagnado *et al*. 1996). Studies with the styryl dye FM1-43 (Betz *et al*. 1996) have yielded estimates of the time-constant for endocytosis as long as *ca*. 20–30 s (Ryan *et al*. 1996; Wu & Betz 1996). This is at least half of the total recycling time—far slower than endocytosis in other secretory systems (Thomas *et al*. 1994; Artalejo *et al*. 1995; Smith & Neher 1997; Engisch & Nowycky 1998). It seems paradoxical that the neurosecretory terminals that might benefit the most from rapid endocytosis do not appear to take advantage of such a mechanism. Does this reflect a genuine difference between the secretory systems, or is it possible that fast retrieval exists in central nerve terminals but is simply not detected by previous applications of the FM1-43 method?

Here we document the existence of fast endocytosis in hippocampal nerve terminals and derive its kinetics from fluorescence measurements using dyes with varying rates of membrane departitioning. The fast endocytotic mechanism we report here possesses several hallmarks of the 'kiss and run' pathway proposed by Bruno Ceccarelli and colleagues (Ceccarelli *et al*. 1973; Ceccarelli & Hurlbut 1980; for review, see Fesce *et al*. 1994). This is a more complete and explanatory presentation of work reported in a recent paper (Klingauf *et al*. 1998).

*Author for correspondence (rwtsien@leland.stanford.edu).
†These authors contributed equally to this work.

2. MATERIALS AND METHODS

(a) *Cell culture*

Hippocampal neurons from CA1–CA3 regions of 2–3-day-old Sprague–Dawley rats were cultured according to previously published protocols (Malgaroli & Tsien 1992; Liu & Tsien 1995) with minor modifications. Cultures were used between two and three weeks *in vitro*.

(b) *Dye loading and destaining*

A modified Tyrode solution (in mM: 150 NaCl, 4 KCl, 2 $MgCl_2$, 2 $CaCl_2$, 10 Glucose, 10 HEPES, pH 7.4) was used as the extracellular medium for all experiments unless noted otherwise. The Tyrode solution always contained 10 µM CNQX to prevent recurrent action potentials. Synaptic boutons were loaded with FM dyes (Molecular Probes, Eugene, OR) in the presence of 45 mM K^+ and 2 mM Ca^{2+} for 90 s at room temperature. Individual boutons were imaged following 15 min of perfusion with dye-free Tyrode's solution. Dye concentrations (2 µM FM1-84, 4 µM FM1-43 and 200µM FM2-10) were chosen to give similar signal intensities.

Solution exchanges for staining and 90 K^+ stimulation were achieved by the fast movement (<200 ms) of an array of micro-capillaries using an MPC-100 programmable micromanipulator (Sutter Instruments, Novato, CA). Flow rate was 1 ml min^{-1}.

Extracellular field stimulation was achieved by 20 mA, 1 ms current pulses through two parallel platinum wires separated by 0.8–1 cm and positioned around the area of interest. Increasing stimulus frequency over the 1–10 Hz range sharply increased the rate of FM dye loss, with no hint of the fall in exocytotic activity found at 40 Hz at frog neuromuscular junctions (Betz & Bewick 1993).

(c) *Optical measurement and analysis*

A computer-controlled optical switch (DX-1000, Stanford Photonics, Palo Alto, CA) was coupled to the epifluorescence port of an inverted Nikon Diaphot TMD microscope via a liquid light guide. For fluorescence imaging we used a Nikon 40×, 1.3 N.A. oil immersion objective. For each data point FM dyes were excited at 480/40 nm (505 DCLP, 535/50 BP) for 66 ms, and two consecutive frames acquired with an intensified progressive line scan CCD camera (Stanford Photonics, Palo Alto, CA). With a duty cycle of two frames per second, we measured a photo-bleaching time-constant of *ca.* 1000 s for all dyes. Accordingly, no corrections of the data for photo-bleaching were made. Images were digitized using board and software from Axon Instruments (Foster City, CA). Circular regions of interest (ROI *ca.* 1.5–2 µm in diameter) were defined around the brightness centre of mass of fluorescence spots. Pixel intensities within an ROI were averaged for each set of two consecutive frames to give one data point. If a displacement of a bouton was observed in subsequent frames, the entire data set was discarded. The relative loss of fluorescence (ΔF) for a given bouton was calculated as the difference between the average of ten data points of baseline before a stimulus and the average of the last ten data points of the time-lapse sequence. Vertical bars denote standard errors of the mean (s.e.m.).

(d) *Modelling*

Exocytosis of releasable vesicles under a sustained stimulus was lumped into a single rate α (cf. figure 8). In the fused state dye could either departition with rate δ or be taken up again by means of fast endocytosis, with rate β. Freshly endocytosed vesicles were recycled back to the readily releasable pool either with a single rate γ (figure 9*b*) or through a series of n consecutive steps each having a rate constant γ/n (figure 9*b*). The variables S_X represent the relative amounts of dye incorporated into vesicular membrane pools, with subscripts 0, 1 and 2 denoting readily releasable, fused, and retrieved vesicles. The state vector $\boldsymbol{S} = (S_0\ S_1\ S_2)^T$ represents the filling of the three states, and its evolution in time is described by the matrix equation

$$\frac{d\boldsymbol{S}}{dt} = \begin{bmatrix} -\alpha & 0 & \gamma \\ \alpha & -(\beta+\delta) & 0 \\ 0 & \beta & -\gamma \end{bmatrix} \boldsymbol{S}$$

The sum of the states S_0, S_1 and S_2 corresponds to the observable fluorescence (F). The amount of retrieved dye can be obtained by integrating the flux through the transition β (figure 8*c*).

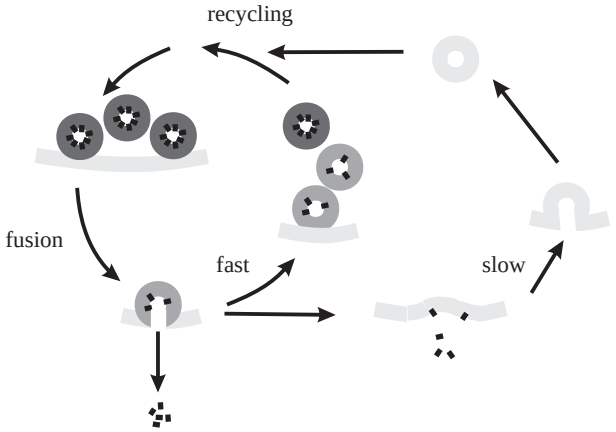

Figure 1. A schematic depiction of recycling of FM dye-marked vesicles. A strong stimulus causes fusion of a large fraction of stained vesicles, followed by dye loss that depends on the rates of endocytosis and dye departitioning. In the classical endocytotic pathway (marked 'slow'), vesicle membrane is retrieved outside the active zone in tens of seconds and should therefore not contain any significant amount of dye. If, however, membrane is retrieved more rapidly at the sites of exocytosis ('fast'), some fraction of dye will be trapped in freshly retrieved vesicles, which will eventually recycle back to the primed pool. Reprinted by permission of *Nature* (Klingauf *et al.* 1998), copyright (1998) Macmillan Magazines Ltd.

3. RESULTS

(a) *Pattern of FM1-43 destaining of synaptic boutons*

Unlike the classical pathway, which is slow enough to allow complete dye loss, a rapid endocytotic mechanism might internalize vesicles before dye had fully departitioned and escaped (figure 1). This could be detected in two ways with fluorescent probes such as FM1-43: first, the initial fluorescence loss would fall far short of completion, no matter how strong the stimulus; second, dye retained by rapid vesicular recapture would continue to mark recycling vesicles but would eventually escape in later exocytotic events, thus supporting delayed destaining.

We have tested these predictions in cultured hippocampal neurons (Malgaroli & Tsien 1992; Liu & Tsien 1995). Presynaptic terminals (boutons) were loaded with FM1-43, washed, then perfused with 90 mM K^+/2 mM

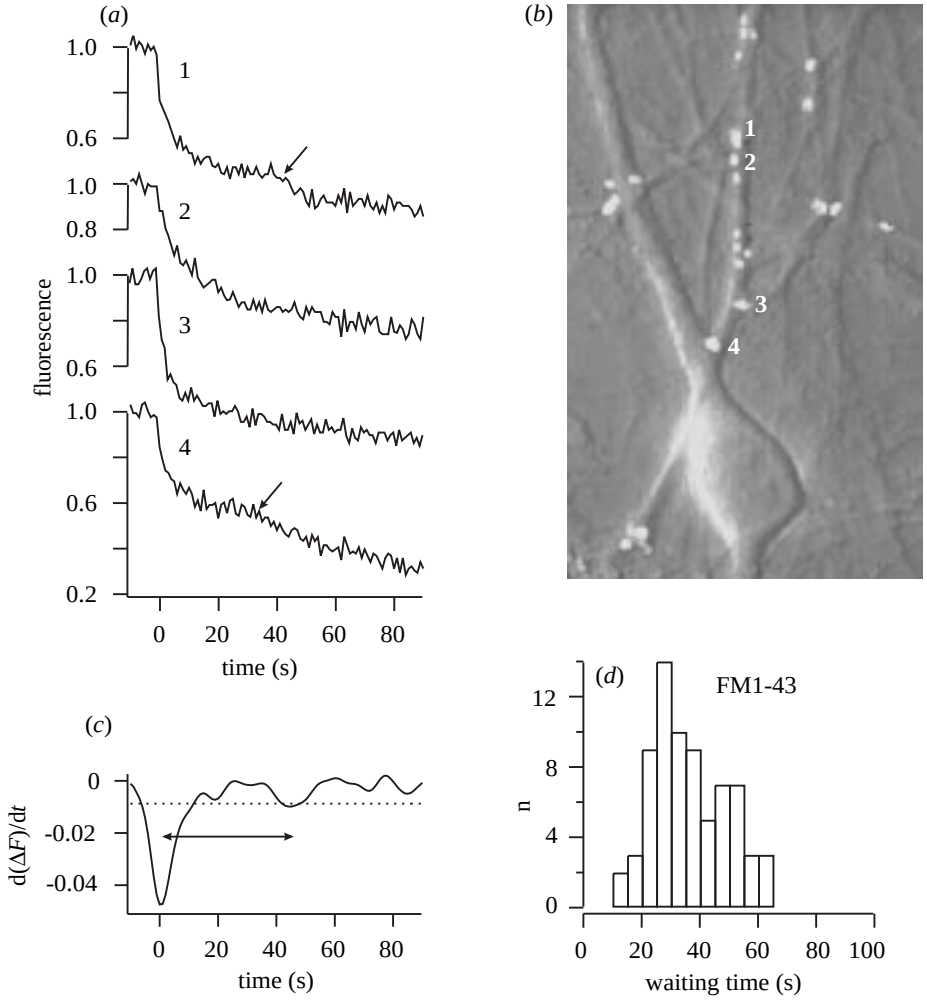

Figure 2. Destaining characteristics of individual synaptic boutons in response to sustained 90 K^+, 2 Ca^{2+}stimulation. (*a*,*b*) Destaining profiles from four FM1-43 loaded boutons, shown in (*b*). Note secondary bursts of destaining (arrows) in traces 1 and 4. (*c*) Secondary bursts of destaining identified in the derivative of the smoothed fluorescence signal. Dotted line illustrates a threshold criterion for secondary bursts, 3 s.d. above baseline fluctuations. (*d*) Waiting time distributions of secondary bursts. Seventy-two out of 191 (37%) FM1-43-stained boutons showed secondary bursts. Reprinted by permission of *Nature* (Klingauf *et al*. 1998), copyright (1998) Macmillan Magazines Ltd.

Ca^{2+} solution to stimulate exocytosis and associated endocytosis (Ryan *et al*. 1993) (figure 2*a*,*b*). The continuous depolarization-induced Ca^{2+} entry caused a markedly biphasic decrease in fluorescence averaged across multiple boutons (figure 2*a*). An initial phase of rapid destaining gave way within seconds to a much more gradual destaining that continued for more than 1 min. This was a consistent finding across a large number of boutons in CA1–CA3 hippocampal cultures, as well as in dentate gyrus–CA3 cultures and cultures obtained from embryonic rat cerebellum (data not shown).

We could exclude a trivial explanation of the biphasic destaining involving inactivation of Ca^{2+} channels and a progressive weakening of the stimulus for exocytosis. Vesicular turnover in hippocampal cultures is supported by presynaptic P/Q- and N-type channels (Reuter 1995; Reid *et al*. 1997), and these are known to undergo voltage-dependent inactivation. To test whether such inactivation might be sufficient to account for the slowed rate of destaining, we carried out the experiment illustrated in figure 3*b*. A set of FM1-43-loaded nerve terminals was subjected to a 30 s exposure to 90 mM K^+, 0-Ca^{2+}, to strongly pre-inactivate presynaptic Ca^{2+} channels, prior to the application of external Ca^{2+} to trigger exocytosis. Despite the pre-inactivation, the fluorescence trace showed the same biphasic pattern of destaining as found without the inactivating predepolarization.

(b) *Analysis of individual dye-stained puncta reveals delayed bursts of destaining*

Destaining profiles of single fluorescent spots provided insight into the basis of the slow phase (figure 2*a*). In any given trial, some puncta displayed a delayed burst of fluorescence loss, seen as a 'kink' in the fluorescence trace (arrows), while others did not. The variability was not explained by incomplete or unreliable superfusion, inasmuch as the full range of responses was found for boutons within a few micrometres of each other (figure 2*b*). Delayed bursts were formally identified as sharp increases in the rate of fluorescence loss, >3 s.d. above background (figure 2*c*). These were found in 37% of the boutons and appeared at a time interval of 20–60 s after the initial drop in fluorescence (figure 2*d*). The mean interval agrees with the *ca*. 40 s period required for recycling of

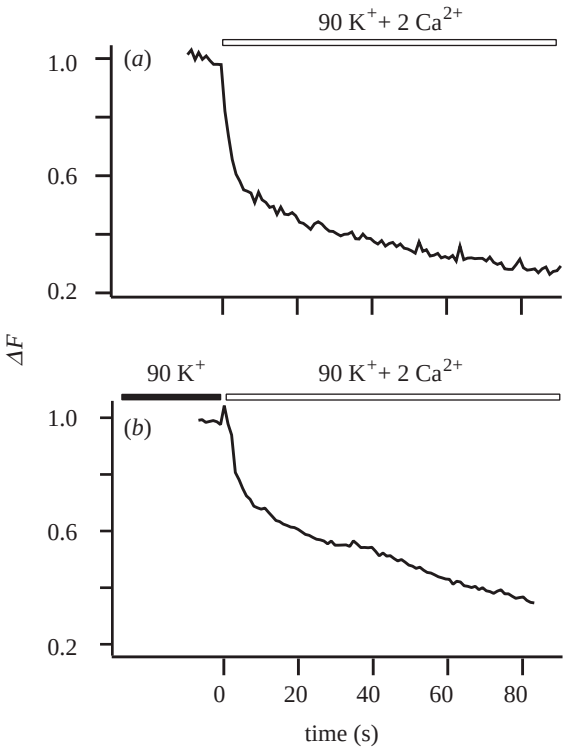

Figure 3. Cumulative destaining characteristics of synaptic puncta (*a*). Ensemble average of destaining profile from all boutons in figure 2*b* displays a biphasic pattern. (*b*) The biphasic destaining was not accounted for by Ca^{2+} channel inactivation: when Ca^{2+} channels were pre-inactivated by a 30 s exposure to high K^+, 0-Ca^{2+}, subsequent admission of Ca^{2+} still caused biphasic destaining.

vesicles that have just undergone exocytosis (Ryan *et al.* 1993; Liu & Tsien 1995; Ryan *et al.* 1996; Lagnado *et al.* 1996).

In some of our experiments, we looked for repeated occurrences of delayed bursts during multiple trials of destaining. Figure 4 illustrates data from a set of seven puncta, obtained during two separate high K^+ challenges, each following an identical loading procedure. The delayed bursts are clearly recognizable in a substantial fraction of records. Some puncta displayed delayed bursts in both the first and second trials, while in other cases, a clear delayed burst was seen in only one trial but not the other. Evidently, the variability seen from one bouton to the next in any given trial (figure 3) reflects a variability that can also be observed at individual boutons during repeated trials (figure 4). The variability in the appearance of the delayed bursts makes sense if one attributes them to the near synchronization of multiple unitary events whose precise timing is stochastic. Whether a clear kink is detected over the background noise depends on the degree of synchronization, and this would be expected to vary randomly in repeated trials. What is most clear is that the timing of the delayed bursts is highly reproducible across multiple boutons and repeated trials. This finding was reinforced by experiments in which nerve terminals were stained with FM2-10, another styryl compound with weaker affinity than FM1-43 for membranes (Betz *et al.* 1996). In this case, the delayed bursts appeared with similar timing, but only in 16% of the traces (Klingauf *et al.* 1998). The lower incidence of clear delayed bursts was as expected if lesser amounts of this dye were retained after the initial round of exocytosis.

(c) *Membrane departitioning time-constants of FM dyes*

FM2-10, FM1-43 and FM1-84 share the same chromophore and differ only in terminal hydrocarbon chain length (2, 4 or 5 carbons, figure 5). Accordingly, these dyes exhibit different rates of membrane dissociation (Ryan *et al.* 1996). The series of dyes offers the potential of serving as temporal callipers for the estimation of the rate of endocytosis. One would expect the more slowly dissociating dyes to show a greater degree of retention in vesicles, if the time required for departitioning were comparable to the duration of the connection between vesicle interior and external milieu. We began by destaining somatodendritic membranes of hippocampal neurons, to check that membrane departitioning followed an exponential time-course (figure 5). The exponential time-constants increased from 0.6–4.7 s with increasing hydrocarbon chain length, a suitably wide range.

The same series of dyes showed significantly different destaining behaviour in hippocampal boutons subjected to continuous depolarization-induced Ca^{2+} entry (figures 6 and 7*a*). The destaining 15 s after initiating the stimulus ranged from 53% for the rapidly departitioning FM2-10, to 46% for FM1-43, to 42% for FM1-84, the slowest of the three probes. The differences in dye loss persisted for many tens of seconds, far longer than any time-constant for dye departitioning, consistent with trapping of dye in internalized vesicles. This was verified by application of multiple stimuli in succession (figure 6*a*). The fluorescence signal hardly changed during the *ca.* 60 s quiescence between stimuli, but dropped immediately upon resumption of depolarization, as expected for a new round of Ca^{2+}-dependent exocytosis from internalized vesicles. Whereas destaining was larger for FM2-10 than FM1-43 during the first trial, it was greater for FM1-43 than for FM2-10 during the second and third trials (figure 6*b*). The pattern of results makes sense in terms of the different rates of departitioning. It would not be expected if the differential retention of dyes were due to a pharmacological effect on some aspect of triggered secretion.

(d) *Activity-dependent regulation of destaining kinetics*

Destaining was less rapid when evoked by field stimulation at 10 Hz (figure 7*b*) than with high K^+, Ca^{2+} stimulation. Nonetheless, the degree of early destaining showed the same systematic variation with the dyes' departitioning kinetics. This reinforced the idea that a significant fraction of synaptic vesicles underwent exocytosis quickly enough to retain dye. With even milder stimulation (1 Hz field stimulation), kinetic distinctions among the three dyes were no longer significant (figure 7*c*,*d*). The results with 1 Hz stimulation are in agreement with Ryan *et al.* (1996).

PHILOSOPHICAL TRANSACTIONS OF THE ROYAL SOCIETY B BIOLOGICAL SCIENCES

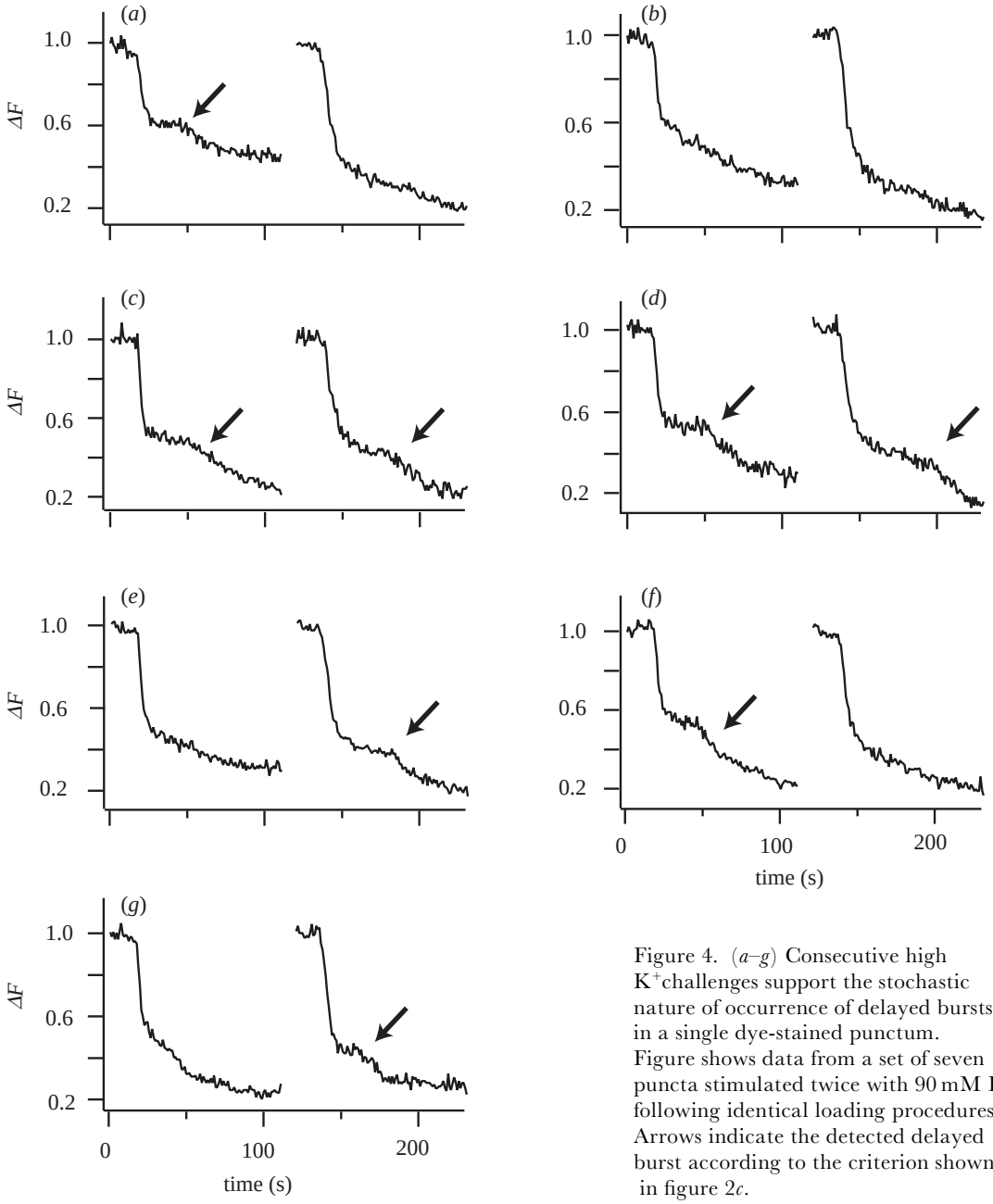

Figure 4. (*a–g*) Consecutive high K^+challenges support the stochastic nature of occurrence of delayed bursts in a single dye-stained punctum. Figure shows data from a set of seven puncta stimulated twice with 90 mM K^+ following identical loading procedures. Arrows indicate the detected delayed burst according to the criterion shown in figure 2*c*.

(e) *Estimation of endocytic rate from dye kinetics*

A simplified kinetic model was constructed (figure 8). The model describes three possible states for fluorescent dye (S_0, S_1 and S_2), defined by the condition of the vesicles that contain the dye (figure 8*a*). The states can be designated as readily releasable (S_0), fused (S_1) and retrieved–reserve (S_2), and are connected in cyclic fashion by the rate constants α, β and γ. The fluorescence can decay by virtue of departitioning of dye from the fused state S_1, according to the rate constant δ (to be set by measured rates of departitioning). The observable fluorescence (F) arises from the sum total of dye in the various vesicle-associated states ($F = S_0 + S_1 + S_2$), whereas dye that has escaped from a membrane environment into the external medium is not detectably fluorescent (Betz *et al.* 1996). A representative kinetic simulation of an FM1-43 destaining experiment that gives a reasonable fit to the experimental data is depicted in figure 8*b*. In this simulation, 60% of the vesicles begin in S_0 and can undergo fusion with τ ($= 1/a$) of 2 s. The fluorescent signal from dye in fused vesicles (S_1) rises initially because of the fusion, but then decays as dye escapes into external medium or is rescued by transition to the retrieved–reserve state. Accordingly, S_2 undergoes a significant initial rise before eventually declining towards zero. In combination, the three components of fluorescence add up to a total that includes a rapid early drop followed by a much slower decay.

Figure 9 compares simulations from the model and experimental data for FM2-10, FM1-43 and FM1-84. The spread between the destaining profiles for the three dyes could be reproduced by setting the rate constant δ according to the observed kinetics for dye departitioning (figure 5). A calculated time-course of destaining for an

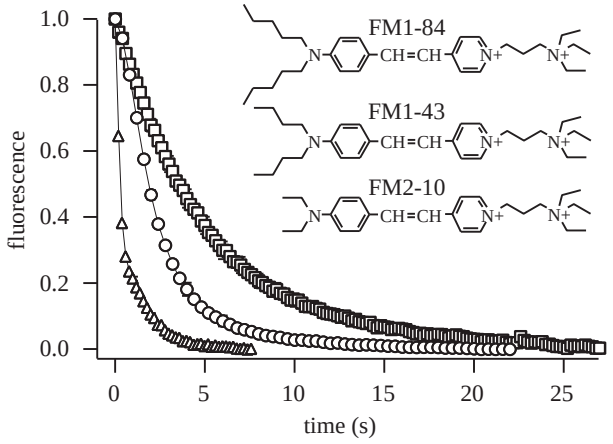

Figure 5. Determination of differences in departitioning kinetics of FM dyes. Departitioning time-constants determined by fast wash-out of equilibrated dyes from neuronal membranes (2mM FM1-84, 4.7 s; 4 mM FM1-43, 2.5 s; 200 mM FM2-10, 0.6 s). Note correlation with alkyl chain length (inset). Reprinted by permission of *Nature* (Klingauf *et al.* 1998), copyright (1998) Macmillan Magazines Ltd.

ideal dye is also shown. The predictions for the time-course of dye destaining and sequestration depended critically on β, the rate of rapid endocytosis. An excellent fit was obtained if we assumed that dye reuptake proceeded with an exponential time-constant of *ca.* 6 s.

A simulation of a delayed burst of destaining was attempted by breaking up the transition γ into smaller steps with the same overall rate (figure 9*b*), thus allowing for a series of events in recycling of retrieved vesicles (Cremona & De Camilli 1997). This modelling captures the defining feature of the delayed burst, an increase in the rate of destaining at a delay interval similar to the independently measured recycling time. The simulation makes no attempt to simulate another distinctive property of the bursts, their stochastic appearance in repeated trials across multiple boutons (figure 4). This may require more complicated schemes, where one takes into account the quantal nature of recycling vesicular membrane and the packets of dye molecules they contain, rather than treating the fluorescent states S_0, S_1 and S_2 simply as continuous variables. The detection of a clear burst will depend critically on the degree of synchronization of vesicular dye packets, hence its stochastic nature. Perhaps further analysis may yield information about the proportion of vesicles that recycle intact, without equilibration with a larger membrane pool (Murthy & Stevens 1998).

(f) *Pharmacological modulation of endocytic rate*

If endocytosis in hippocampal terminals proceeds several-fold faster than previously thought, might it be further accelerated by modulatory mechanisms? Staurosporine, a broad-spectrum protein kinase inhibitor was of particular interest. At neuromuscular junctions, staurosporine has been reported to eliminate FM1-43 destaining without affecting quantal acetylcholine release (Henkel & Betz 1995). At terminals of cultured hippocampal neurons, staurosporine reduces FM1-43 loss (Kraszewski *et al.* 1996). These findings have been somewhat controversial, with some groups finding little or no effect of this

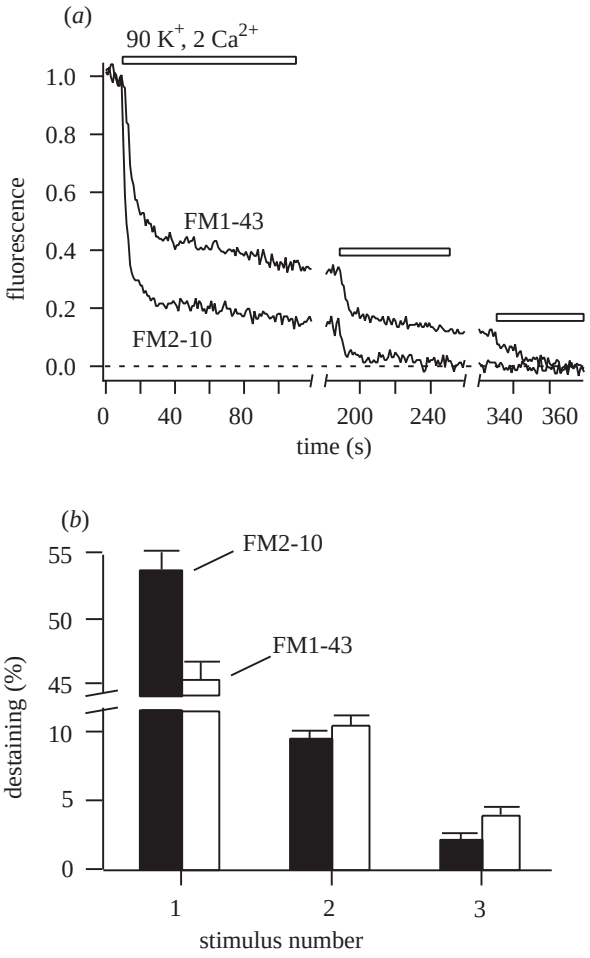

Figure 6. Differences in departitioning kinetics of FM dyes support detection of fast endocytosis. (*a*) Smaller amplitudes of initial destaining for FM1-43 compared to FM2-10 indicate reinternalization of FM1-43. (*b*) Comparison of amplitudes of destaining, 15 s following stimulation, for multiple rounds of stimuli (first round $53.3 \pm 0.01\%$ versus $46.5 \pm 0.01\%$ for FM2-10 ($n = 90$) and FM1-43 ($n = 87$) respectively, $p < 0.0001$; second round $9.3 \pm 0.007\%$ versus $10.5 \pm 0.005\%$, $p = 0.07$; third round $2.1 \pm 0.004\%$ versus $4.1 \pm 0.003\%$ $p < 0.001$). Reprinted by permission of *Nature* (Klingauf *et al.* 1998), copyright (1998) Macmillan Magazines Ltd.

agent. Accordingly, we looked for possible effects of staurosporine on endocytosis using the quantitative approach presented here (figure 10*a*,*b*). Preincubation with staurosporine produced a striking diminution of the initial loss of FM1-43 (figure 10*a*) and FM2-10 (figure 10*b*), without any significant effect on the total amount of dye release. Both sets of data could be accounted for by speeding the endocytotic rate constant by *ca.* threefold (smooth curves; β^{-1} reduced from 6 s to *ca.* 1.7 s in staurosporine). In contrast, simulated effects of various changes in exocytotic rate did not fit the data (slowly declining curve). Thus, the kinetics of endocytosis seem to be subject to modulatory control.

(g) *Ca^{2+}-dependent regulation of fast endocytosis*

Additional controversy surrounds effects of elevated Ca^{2+} on endocytosis. In secretory cells, increases in internal Ca^{2+} are generally found to accelerate endocytosis (Thomas *et al.* 1994; Parsons *et al.* 1994; Burgoyne

PHILOSOPHICAL TRANSACTIONS OF THE ROYAL SOCIETY B BIOLOGICAL SCIENCES

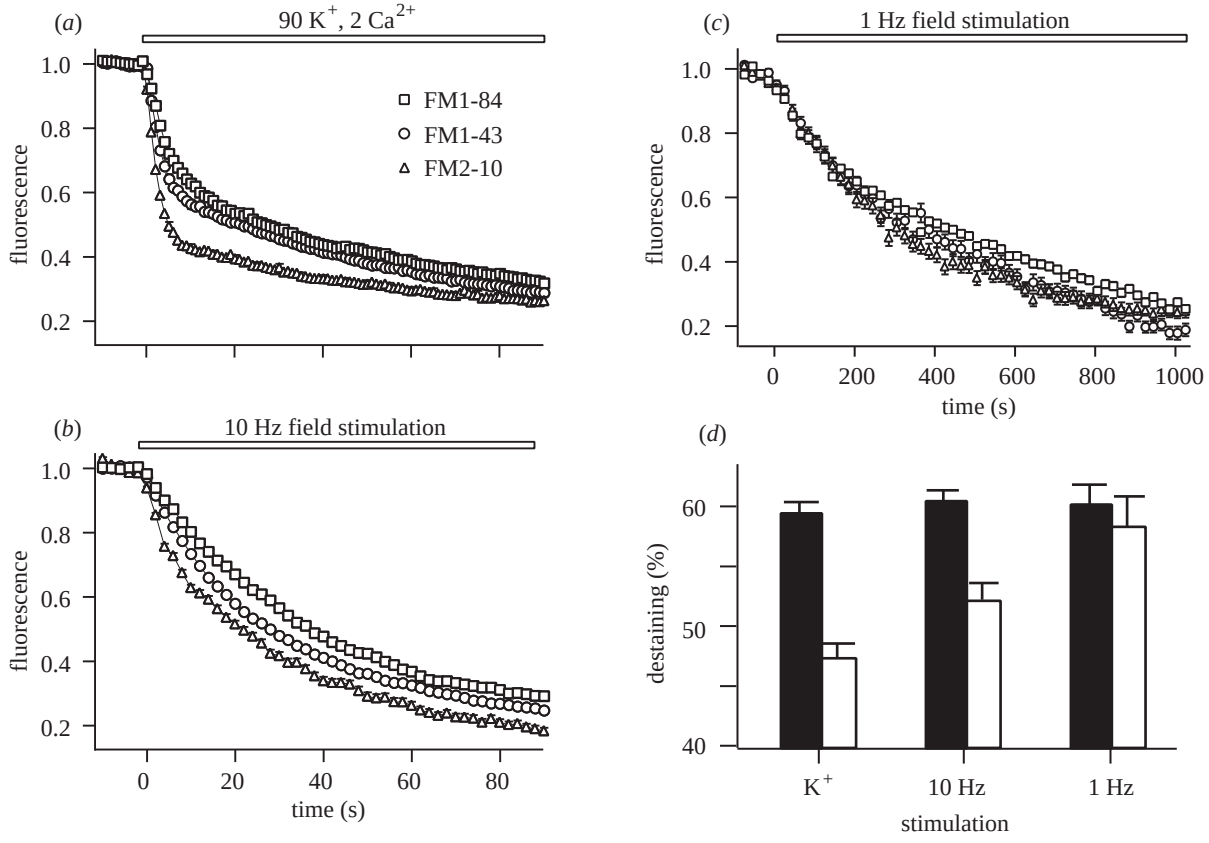

Figure 7. Alterations in destaining kinetics in response to changing stimulus pattern. (*a*) Ensemble averages of destaining profiles with 2 mM FM1-84, 4 mM FM1-43 and 200 mM FM2-10 ($n = 92$, $n = 90$ and $n = 87$ boutons). The residual fluorescence at the end of a fourth trial (not shown) was taken as baseline. (*b*) Differences in destaining kinetics with 10 Hz extracellular field stimulation ($n = 120$ for FM1-84, $n = 102$ for FM 1-43, $n = 89$ for FM2-10). Background fluorescence was determined following several applications of 90 K^+/2 Ca^{2+} solution. (*c*) Destaining kinetics with 1 Hz field stimulation do not exhibit significant differences among FM dyes ($n = 112$ for FM1-84, $n = 40$ for FM1-43, $n = 44$ for FM2-10). Experimental paradigm is the same as in *b*. (*d*) Degree of FM1-43 destaining (open bars) when FM2-10 fluorescence loss (filled bars) was *ca.* 60% (47.5 ± 1.3% for 90 K^+ stimulation, 52.3 ± 1.1% for 10 Hz, 58.5 ± 2.5% for 1 Hz). Reprinted by permission of *Nature* (Klingauf *et al.* 1998), copyright (1998) Macmillan Magazines Ltd.

1995; Smith & Neher 1997; Plattner *et al.* 1997), although one study reports that high $[Ca^{2+}]_i$ has the opposite effect (von Gersdorff & Matthews 1994). Endocytosis at *Drosophila* neuromuscular junctions shows an absolute requirement for Ca^{2+} (Ramaswani *et al.* 1994), whereas no requirement for $[Ca^{2+}]_0$ was found at hippocampal boutons (Ryan *et al.* 1996). Accordingly, we explored effects of varying $[Ca^{2+}]_0$ under conditions where fast endocytosis was prominent (figure 11*a*,*b*). Raising $[Ca^{2+}]_0$ from 1 to 8 mM significantly decreased the initial release of FM2-10 (figure 11*a*,*b*), corresponding to speeding of fast endocytosis from *ca.* 8 s to *ca.* 2 s. This observation is the opposite of what one would expect if dye destaining profile solely reflected exocytosis. The Ca^{2+}-dependent increase in the rate of exocytosis seems to dominate at lower $[Ca^{2+}]_0$, whereas at higher $[Ca^{2+}]_0$, a concomitant increase in the rate of endocytosis actually slows destaining. The slower probes FM1-43 and FM1-84 were also increasingly retained as $[Ca^{2+}]_0$ was elevated (figure 11*b*), although the degree of retention levelled off at *ca.* 60% (no less than *ca.* 40% untrapped fluorescence even at high Ca^{2+}). Dye trapping by fast vesicle retrieval would be expected to reach a ceiling once its rate greatly exceeded the rate of dye departitioning. The remaining 40% fluorescence loss provides a clue that a substantial fraction of vesicles may be shunted away from rapid endocytosis into a slow endocytotic pathway where vesicles completely destain while awaiting retrieval (figure 1) (Kraszewski *et al.* 1996).

4. DISCUSSION

Our results have demonstrated the existence of rapid endocytosis of vesicles at synapses between hippocampal neurons. The retrieval was swift enough to prevent complete loss of FM1-43 during an initial round of exocytosis. FM dyes with longer hydrocarbon tails were retained to increasing degrees in precise relationship to their measured departitioning rates. The series of dyes provided kinetic information presently unattainable with capacitance measurements, and distinct from that derived from synaptic currents, which mark precisely the moment of fusion pore opening and transmitter efflux but give no direct information about the timing of endocytosis. Our estimates of the endocytotic time-constant ranged from *ca.* 6 s under normal recording conditions down to < 2 s under modulation, an order of magnitude faster than previous estimates at hippocampal synapses. If anything,

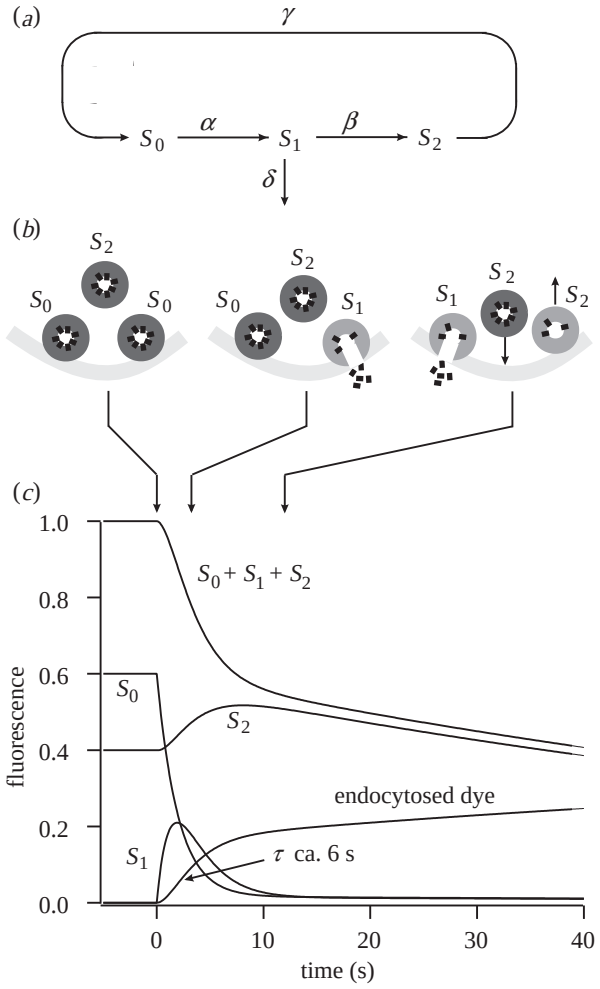

Figure 8. A simple model accounts for the dependence of bouton destaining kinetics on dye species. Modelling of dye destaining during sustained stimulation. The observable fluorescence ($F = S_0+S_1+S_2$) arises from dye in readily releasable (S_0), fused (S_1) and retrieved (S_2) vesicles. Reprinted by permission of *Nature* (Klingauf *et al.* 1998), copyright (1998) Macmillan Magazines Ltd.

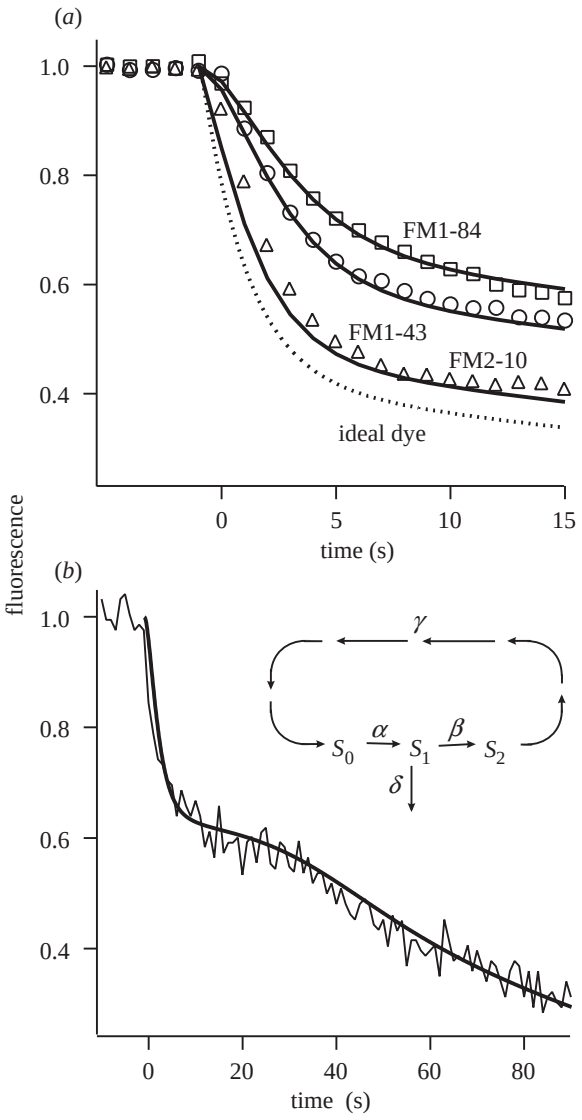

Figure 9. Kinetic simulations of experimental data from figure 7*a*. (*a*) In the best fit, $\alpha = 0.5\,s^{-1}$, $\gamma = 0.014\,s^{-1}$ and $\beta = 0.167\,s^{-1}$, giving a time-constant of fast endocytosis of 6 s. δ was set by measured rates of departitioning (figure 5). 60% of the vesicles were assumed readily releasable. (*b*) Simulation of a 'kink' by assuming six consecutive steps for vesicle recycling ($\alpha = 0.5\,s^{-1}$, $\beta = 0.5\,s^{-1}$, $\delta = 0.4\,s^{-1}$ and each $\gamma = 0.142\,s^{-1}$). The dye content of the releasable pool (S_0) was set at an initial value of 80%, and the intermediate states leading up to S_0 were initially evenly populated. Reprinted by permission of *Nature* (Klingauf *et al.* 1998), copyright (1998) Macmillan Magazines Ltd.

the maximum speed of rapid endocytosis may be underestimated since the kinetic model lumps it together with any slow internalization working in parallel.

The incompleteness of the initial dye loss has another important implication: at the moment of fusion there cannot be free lateral diffusion of dye from vesicle to plasmalemma. This suggests that lipid phases of vesicle and plasma membrane are not initially continuous, but must be restricted by a barrier. The barrier could be the fusion pore itself (Zimmerberg *et al.* 1994). The vesicle membrane must remain segregated from internal membrane organelles, at least in large part. The common occurrence of delayed bursts of destaining supports the idea that a large percentage of internalized vesicles recycle intact (Murthy & Stevens 1998), possibly via a 'kiss and run' mechanism (Ceccarelli & Hurlbut 1980; Fesce *et al.* 1994) or by clathrin-mediated, non-endosomal retrieval (Takei *et al.* 1996).

Our experiments suggest that the rate of rapid endocytosis increases with stimulus strength and elevated $[Ca^{2+}]_i$, thus bringing hippocampal nerve terminals in line with certain non-neuronal secretory systems (Henkel & Almers 1996; Smith & Neher 1997). The rapid endocytosis at higher stimulus frequencies described here (figure 7*b*) fits nicely with results from an earlier study by Ryan *et al.* (1996), showing a sharp drop in the ability of hippocampal nerve terminals to take up FM1-43 just 5 s after cessation of 10 Hz stimulation. The ability of staurosporine to inhibit FM dye release (Henkel & Betz 1995; Kraszewski *et al.* 1996) can be explained by a decrease in the time that vesicular membrane is externally accessible (Henkel & Betz 1995) relative to that in the absence of drug (Betz & Bewick 1993) (figure 10*a*,*b*). This effect of staurosporine may actually be targeting an endogenous protein kinase C-dependent pathway that

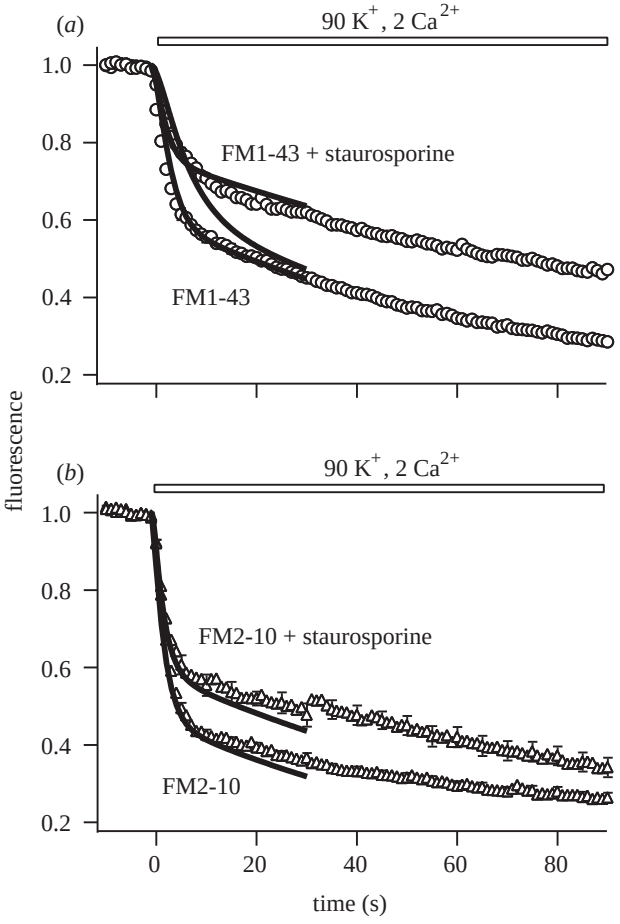

Figure 10. Effects of staurosporine and elevated $[Ca^{2+}]_0$. (*a*, *b*) Ensemble averages of FM1-43 (*a*) and FM2-10 (*b*) destaining profiles from boutons pre-treated for 1 h with 2 μM staurosporine (top, $n = 95$ for FM1-43, $n = 98$ for FM2-10) or DMSO only (bottom). Smooth curves were simulated by changing only the endocytotic time constant (β^{-1}), from 6 s (control) to 1.7 s (staurosporine). The middle line was simulated by slowing exocytosis threefold. Reprinted by permission of *Nature* (Klingauf *et al*. 1998), copyright (1998) Macmillan Magazines Ltd.

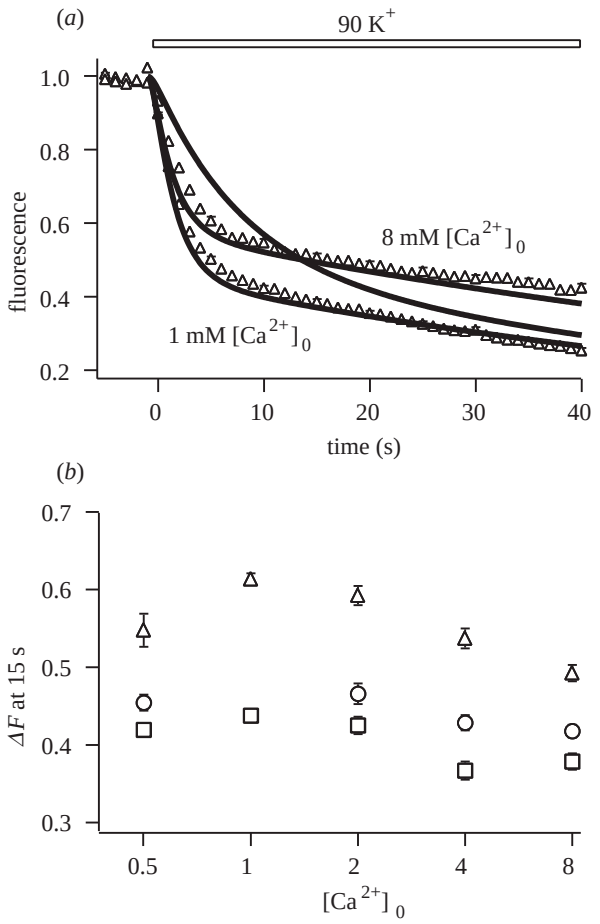

Figure 11. Slowing of dye destaining kinetics with increasing external Ca^{2+}. (*a*) FM2-10 destaining kinetics in 1 mM and 8 mM $[Ca^{2+}]_0$. The model fit the data when the endocytotic time-constant was reduced from 8 s to 1.7 s, while a change of the exocytotic rate α (from 0.5 s^{-1} to 0.125 s^{-1}) did not produce a good fit (middle trace). (*b*) Summary of destaining experiments with elevated $[Ca^{2+}]_0$. Each data point indicates the mean fluorescence loss at 15 s (*ca*. three times the longest departitioning time-constant) following 90 K^+stimulation. Symbols as in figures 5 and 7. Reprinted by permission of *Nature* (Klingauf *et al*. 1998), copyright (1998) Macmillan Magazines Ltd.

regulates the exocytotic fusion pore kinetics (Scepek *et* al. 1998). The lack of effect of staurosporine on antibody uptake (Kraszewski *et al*. 1996) also makes sense if this uptake largely involves a slow internalization pathway rather than fast retrieval.

Finding that nerve terminals of CNS neurons can make use of efficient mechanisms for rapid vesicular retrieval opens up new possibilities for how synaptic communication in the brain might be regulated. This regulation can be achieved through the Ca^{2+} and/or staurosporine-dependent pathways we examined here. However, the nature of physiological stimuli that can activate these pathways remains to be determined. Modulation of endocytic rate is clearly advantageous in sustaining balance between vesicular delivery and recycling, and may be important for control of vesicle availability (see also Wang & Kaczmarek 1998).

We thank Stephen J. Smith and Thomas L. Schwarz for critically reading an earlier version of the manuscript. We thank Jeremy Bergsman for helpful discussions and suggestions throughout this study. This work was supported by grants from NIMH, the Mathers Charitable Foundation, the McKnight Endowment Fund for Neuroscience (R.W.T.), and fellowships from the American Heart Association California Affiliate (E.T.K.) and the Boehringer Ingelheim Fonds (J.K.).

REFERENCES

Artalejo, C. R., Henley, J. R., McNiven, M. A. & Palfrey, H. C. 1995 Rapid endocytosis coupled to exocytosis in adrenal chromaffin cells involves Ca^{2+}, GTP, and dynamin but not clathrin. *Proc. Natn. Acad. Sci. USA* **92**, 8328–8332.

Betz, W. J. & Bewick, G. S. 1993 Optical monitoring of transmitter release and synaptic vesicle recycling at the frog neuromuscular junction. *J. Physiol. (Lond.)* **460**, 287–309.

Betz, W. J., Mao, F. & Smith, C. B. 1996 Imaging exocytosis and endocytosis. *Curr. Opin. Neurobiol.* **6**, 365–371.

Burgoyne, R. D. 1995 Fast exocytosis and endocytosis triggered by depolarisation in single adrenal chromaffin cells before rapid Ca^{2+} current run-down. *Pflügers Arch.* **430**, 213–219.

Ceccarelli, B. & Hurlbut, W. P. 1980 Ca^{2+}-dependent recycling of synaptic vesicles at the frog neuromuscular junction. *J. Cell Biol.* **87**, 297–303.

Ceccarelli, B., Hurlbut, W. P. & Mauro, A. 1973 Turnover of transmitter and synaptic vesicles at the frog neuromuscular junction. *J. Cell Biol.* **57**, 499–524.

Cremona, O. & De Camilli, P. 1997 Synaptic vesicle endocytosis. *Curr. Opin. Neurobiol.* **7**, 323–330.

Engisch, K. L. & Nowycky, M. 1998 Compensatory and excess retrieval: two types of endocytosis following single step depolarizations in bovine adrenal chromaffin cells. *J. Physiol.* **506**, 591–608.

Fesce, R., Grohovaz, F., Valtorta, F. & Meldolesi, J. 1994 Neurotransmitter release: fusion or 'kiss and run'? *Trends Cell Biol.* **4**, 1–4.

Harris, K. M. & Sultan, P. 1995 Variation in the number, location and size of synaptic vesicles provides an anatomical basis for the nonuniform probability of release at hippocampal CA1 synapses. *Neuropharmacology* **34**, 1387–1395.

Henkel, A. W. & Almers, W. 1996 Fast steps in exocytosis and endocytosis studied by capacitance measurements in endocrine cells. *Curr. Opin. Neurobiol.* **6**, 350–357.

Henkel, A. W. & Betz, W. J. 1995 Staurosporine blocks evoked release of FM1-43 but not acetylcholine from frog motor nerve terminals. *J. Neurosci.* **15**, 8246–8258.

Heuser, J. E. & Reese, T. S. 1973 Evidence for recycling of synaptic vesicle membrane during transmitter release at the frog neuromuscular junction. *J. Cell Biol.* **57**, 315–344.

Klingauf, J., Kavalali, E. T. & Tsien, R. W. 1998 Kinetics and regulation of fast endocytosis at hippocampal synapses. *Nature* **394**, 581–585.

Koenig, J. H. & Ikeda, K. 1996 Synaptic vesicles have two distinct recycling pathways. *J. Cell Biol.* **135**, 797–808.

Kraszewski, K., Daniell, L., Mundigl, O. & De Camilli, P. 1996 Mobility of synaptic vesicles in nerve endings monitored by recovery from photobleaching of synaptic vesicle-associated fluorescence. *J. Neurosci.* **16**, 5905–5913.

Lagnado, L., Gomis, A. & Job, C. 1996 Continuous vesicle cycling in the synaptic terminal of retinal bipolar cells. *Neuron* **17**, 957–967.

Liu, G. & Tsien, R. W. 1995 Properties of synaptic transmission at single hippocampal synaptic boutons. *Nature* **268**, 1624–1628.

Malgaroli, A. & Tsien, R. W. 1992 Glutamate-induced long-term potentiation of the frequency of miniature synaptic currents in cultured hippocampal neurons. *Nature* **357**, 134–139.

Miller, T. M. & Heuser, J. E. 1984 Endocytosis of synaptic vesicle membrane at the frog neuromuscular junction. *J. Cell Biol.* **98**, 685–698.

Murthy, V. N. & Stevens, C. F. 1998 Synaptic vesicles retain their identity through the endocytotic cycle. *Nature* **392**, 497–501.

Parsons, T. D., Lenzi, D., Almers, W. & Roberts, W. M. 1994 Calcium-triggered exocytosis and endocytosis in an isolated presynaptic cell: capacitance measurements in saccular hair cells. *Neuron* **13**, 875–883.

Plattner, H., Braun, C. & Hentschel, J. 1997 Facilitation of membrane fusion during exocytosis and exocytosis-coupled endocytosis and acceleration of 'ghost' detachment in *Paramecium* by extracellular calcium. A quenched-flow/freeze-fracture analysis. *J. Membr. Biol.* **158**, 197–208.

Ramaswami, M., Krishnan, K. S. & Kelly, R. B. 1994 Intermediates in synaptic vesicle recycling revealed by optical imaging of *Drosophila* neuromuscular junctions. *Neuron* **13**, 363–375.

Reid, C. A., Clements, J. D. & Bekkers, J. M. 1997 Nonuniform distribution of Ca^{2+} channel subtypes on presynaptic terminals of excitatory synapses in hippocampal cultures. *J. Neurosci.* **17**, 2738–2745.

Reuter, H. 1995 Measurements of exocytosis from single presynaptic nerve terminals reveal heterogeneous inhibition by $Ca^{(2+)}$-channel blockers. *Neuron* **14**, 773–779.

Ryan, T. A., Reuter, H., Wendland, B., Schweizer, F. E., Tsien, R. W. & Smith, S. J. 1993 The kinetics of synaptic vesicle recycling measured at single presynaptic boutons. *Neuron* **11**, 713–724.

Ryan, T. A., Smith, S. J. & Reuter, H. 1996 The timing of synaptic vesicle endocytosis. *Proc. Natn. Acad. Sci. USA* **93**, 5567–5571.

Scepek, S., Coorssen, J. R. & Lindau, M. 1998 Fusion pore expansion in horse eosinophils is modulated by Ca^{2+} and protein kinase C via distinct mechanisms. *EMBO J.* **17**, 4340–4345.

Schikorski, T. & Stevens, C. F. 1997 Quantitative ultrastructural analysis of hippocampal excitatory synapses. *J. Neurosci.* **17**, 5858–5867.

Smith, C. & Neher, E. 1997 Multiple forms of endocytosis in bovine adrenal chromaffin cells. *J. Cell Biol.* **139**, 885–894.

Takei, K., Mundigl, O., Daniell, L. & De Camilli, P. 1996 The synaptic vesicle cycle: a single vesicle budding step involving clathrin and dynamin. *J. Cell Biol.* **133**, 1237–1250.

Thomas, P., Lee, A. K., Wong, J. G. & Almers, W. 1994 A triggered mechanism retrieves membrane in seconds after $Ca^{(2+)}$-stimulated exocytosis in single pituitary cells. *J. Cell Biol.* **124**, 667–675.

von Gersdorff, H. & Matthews, G. 1994 Inhibition of endocytosis by elevated internal calcium in a synaptic terminal. *Nature* **370**, 652–655.

Wang, L. Y. & Kaczmarek, L. K. 1998 High-frequency firing helps replenish the readily releasable pool of synaptic vesicles. *Nature* **394**, 384–388.

Wu, L. G. & Betz, W. J. 1996 Nerve activity but not intracellular calcium determines the time course of endocytosis at the frog neuromuscular junction. *Neuron* **17**, 769–779.

Zimmerberg, J., Blumenthal, R., Sarkar, D. P., Curran, M. & Morris, S. J. 1994 Restricted movement of lipid and aqueous dyes through pores formed by influenza hemagglutinin during cell fusion. *J. Cell Biol.* **1271**, 885–894.

PHILOSOPHICAL TRANSACTIONS OF THE ROYAL SOCIETY B BIOLOGICAL SCIENCES